Soler, M., Kamgarpour, M., Lloret, J. y Lygeros, J. (2016). A Hybrid Optimal Control Approach to Fuel Efficient Aircraft Conflict Avoidance. *IEEE Transactions on Intelligent Transportation Systems*, 17(7), pp. 1826 - 1838.

DOI: https://doi.org/10.1109/TITS.2015.2510824

A Hybrid Optimal Control Approach to Fuel Efficient Aircraft Conflict Avoidance

Manuel Soler, Maryam Kamgarpour, Javier Lloret, and John Lygeros, *Fellow, IEEE*

***Abstract*—We formulate fuel optimal conflict free aircraft trajectory planning as a hybrid optimal control problem. The discrete modes of the hybrid system capture the air traffic procedures for conflict resolution, e. g., speed and turn advisories. In order to solve problems of realistic dimensions arising from air traffic sector planning, we formulate a numerically tractable approach to solve the hybrid optimal control problem. The approach is based on introducing binary functions for each mode, relaxing the binary functions and including a penalty term on the relaxation. The transformed and discretized problem is a nonlinear program. We use the approach on a realistic case study with 7 aircraft within an air traffic control sector, in which we find minimum fuel conflict free trajectories.**

***Index Terms*—hybrid optimal control, conflict detection and resolution algorithms, air traffic control**

I. Introduction

AIR Traffic Management (ATM) is responsible for safe, efficient and sustainable operation in civil aviation. Since its birth in the 1920s, the ATM system has evolved from its primitive form that consisted of a set of simple operation rules to its current version that is a complex network of management layers, communication, navigation, and surveillance subsystems. A paradigm shift in the current ATM system is being pursued to address the continuous growth of air traffic demand, high fuel prices and growing concerns over the environmental impact of air transportation [1], [2].

Currently, ATM imposes certain trajectory restrictions to guarantee safety and to ease the task of air traffic control operators (ATCOs). Some of these restrictions result in non-minimal fuel consumptions and hence higher operating costs and emissions. The future ATM is envisioned to be built around the so called Trajectory Based Operational (TBO) concept, which would allow aircraft more freedom to optimize their trajectories according to airlines' business interests. An important problem in implementing the TBO concept is designing trajectories that are optimal with respect to a cost function, while being safe in the presence of hazardous weather and other aircraft. Moreover, in the future ATM the ATCOs would still be in the loop, and thus trajectories should also be *cognitive friendly*. This ensures high levels of efficiency and safety via automation, yet accounts for human's trust and acceptance. In this work, we propose an optimal control framework, consistent with the operational procedures of ATCOs, pilots and autopilots, for minimum fuel conflict resolution in pre-tactical (20 minutes to one hour) trajectory planning.

Aircraft conflict detection and resolution has been studied extensively [3], [4], [5]. Here, we briefly discuss some of the most relevant approaches to our proposed framework. Algorithms based on mixed integer linear program (MILP) [6], [7], [8], [9] considered conflict resolution through speed, heading, altitude maneuvers, or a combination of them. In [10] integer variables are introduced for defining priorities on aircraft deviations from their nominal trajectories, resulting in a MILP. Despite well-studied theoretical and computational results of MILP, a disadvantage of this approach is that aircraft dynamics need to be approximated by linear models. Nonlinearities have been tackled, resulting in conflict detection and resolution algorithms based on mixed integer nonlinear programs (MINLP) [11], [12] or a hybridization of MILP and nonlinear program (NLP) [13]. While the nonlinear formulations above model the aircraft dynamics more accurately than the linearized counterparts, a complete 3-Degree-of-Freedom (DoF) model (including mass variation) is not captured. Thus, the fidelity of the solution with regards to performances and fuel consumption is limited using these approaches.

Motivated by the free routing possibilities that may arise due to the TBO concept, optimal control is used for conflict free trajectory planning [14] based on a kinematic model of the aircraft motion. In [15] genetic algorithms are used to plan conflict free and optimized flight paths, given general cost functions. Here, discrete decision variables of waypoint addition and heading selection are optimized through an evolutionary process. The advantage is the speed of convergence of these algorithms to optimal solutions with high probabilities. A difficulty is that to consider full nonlinear 3DoF equations of motion to synthesize a continuous trajectory, a large number of discretized optimization variables may need to be introduced and this reduces the computational efficiency. A typical strategy to tackle optimal control problems with more realistic dynamics and constraints is to use the so-called direct methods [16] through discretization of the optimal control problem and obtaining a Nonlinear Program (NLP). This strategy was used in [17] to design minimum-time conflict free trajectories.

Despite several advances, algorithms capable of accounting for (1) accurate 3 DoF flight dynamics models and at the

M. Soler (assistant prof.) and J. Lloret (part time lecturer) are with the Department of Bioengineering and Aerospace Engineering, UC3M, 28911 Madrid, Spain, {masolera@ing.uc3m.es}. J. Lloret {javier.lloret@uc3m.es} works full time as Air Traffic Controller at AENA.

M. Kamgarpour (postdoc fellow) and J. Lygeros (full prof.) are with the Department of Electrical Engineering and Information Technology, ETH Zurich, {mkamgar,lygeros@control.ee.ethz.ch}.

Final version submitted on Dec 18, 2015. This paper corresponds to the accepted version of paper with DOI: 10.1109/TITS.2015.2510824. Paper supported by the *Spanish Ministry of Economy and Competitiveness* via project TRA2014-58413-C2-2-R.

same time (2) maneuvers consistent with the current air traffic control (ATC) procedures have not been fully explored. To address this issue, we consider a hybrid optimal control framework that can accurately capture aircraft dynamics [18], [19], [20]. A hybrid dynamical model combines continuous state dynamics with discrete states, also referred to as modes of operation. In this framework, the discrete states represent the flight modes and operating procedures, whereas the continuous states describe dynamic variables such as position and speed. The task of safe and optimal trajectory design can then be formulated as an optimal control problem for a hybrid system subject to flight envelope and collision avoidance constraints.

The hybrid optimal control problem with a known mode sequence is referred to as a multiphase optimal control problem in the aerospace community. In [21], [22], multiphase optimal control has been used to optimize trajectory of a single civilian aircraft resulting in significant reduction in fuel consumption compared to current procedures. Nevertheless, for conflict free trajectory planning the number of mode switches, corresponding to the number of advisories in ATC context, and the sequence of active modes, corresponding to type of advisories, that resolve a conflicting aircraft scenario while minimizing fuel consumption are not known *a priori*.

Recently, we addressed conflict free trajectory planning with a pre-fixed number of advisories for each aircraft and found the types of advisories that result in an optimal resolution strategy. The problem was formulated as a mixed-integer optimal control problem (MIOCP for short) [23], [24]. Through discretization, the MIOCP was approximated by a MINLP [25], [26] and solved via Branch & Bound techniques. Using this approach, fuel optimized conflict free trajectories for two aircraft planar encounter were derived [27]. This approach has two limitations that we will address in this paper. First, the MINLP becomes quickly intractable as the number of binary variables increases, and so the number of aircraft that can be considered in a scenario is very limited. Second, the number of mode switches (number of advisories) must be set *a priori*.

The hybrid optimal control problem with an unknown number and sequence of modes is a challenging open problem. Several approaches are developed which differ based on assumptions on dynamics [28], or the underlying approach (hybrid dynamic programming [29], hybrid Maximum Principle [30], [31], [32], two stage algorithms [33], [34]). An alternative approach is to relax the binary functions associated to the mode sequence to obtain a convexification or embedding of binary constraints [35], [36], [37]. Here, a mode sequence corresponds to a Bang-Bang solution in the relaxed formulation. A challenge with this approach is to project back a relaxed solution to a discrete sequence of modes. There is no optimal way of defining this mapping and in general, the constraints may not be satisfied after the projection. In this paper, we consider this relaxation of the binary mode sequence but tackle the ambiguity in projection of relaxed solution as follows. We introduce a penalty function in order to penalize solutions that are non-binary. We prove convergence of the relaxed solutions with sufficiently high penalty weight to binary solutions and thus, remove the need for the projection of solution.

Summarizing the above discussions, our methodology is as follows. First, we formulate fuel optimal conflict free aircraft trajectory planning as a hybrid optimal control problem with accurate aircraft dynamics and two modes that account for speed and turn advisories. Second, we cast the hybrid optimal control problem into a classical optimal control problem through a relaxation of integer constraints and addition of a penalty term on the relaxation. The fundamental contribution of the paper is the application of our formulation and solution approach to a realistic case study with 7 aircraft within an ATC sector in Spain. We find minimum fuel, de-conflicted trajectories compatible with ATC advisories. Note that a preliminary formulation was presented in [38], in which the canonical *roundabout configuration* was considered. By solving a realistic case based on ATC data, we further contribute with an in-depth ATC based operational analysis and discuss current situation and future trends.

This work is organized as follows: In Section II we define the hybrid optimal control problem and describe how it models the aircraft trajectory planning problem. In Section III we describe our solution method. In Section IV we formulate the aircraft fuel optimization as a constrained hybrid optimal control problem. In Section V we present a detailed case study based on a realistic scenario in an ATC sector. In addition, we compare the optimized solution with the current procedures. In Section VI we summarize and discuss future work.

II. Hybrid Optimal Control

Flight dynamics of an aircraft can be described by a switched dynamical system, that is, a dynamical system with multiple modes of operation. These modes denote for instance climb/descend maneuvers, acceleration/deceleration maneuvers, and turn maneuvers. Each flight mode is characterized by a different set of differential equations and constraints. As such, we consider a switched system described by a set of differential equations

$$\dot{x}(t) = f_q(x(t), u(t)),\ q \in Q := \{1, 2, \ldots, n_q\}, \qquad (1)$$

where $x(t) \in \mathbb{R}^{n_x}$ represents the continuous states, $f_q : \mathbb{R}^{n_x} \times \mathbb{R}^{n_u} \to \mathbb{R}^{n_x}$ represents the dynamics in mode q, and n_q represents the number of discrete modes. The input $u(t)$ is in a compact set $U \subset \mathbb{R}^{n_u}$. For aircraft flight, x denotes the dynamic states of the aircraft, e.g., position and speed, and u denotes the control variables, e.g., throttle level position.

A switching sequence σ is defined as the timed sequence of active dynamical systems, or modes, as follows:

$$\sigma = [(t_0, q_0), (t_1, q_1), \ldots, (t_N, q_N)],$$

where N represents the number of mode switches (considering also the final time as a switch), and $q_i \in Q$ for $i = 0, 1, \ldots, N$. t_0 is the initial time, t_i for $i = 1, \ldots, N$, with $t_0 \leq t_1 \leq \cdots \leq t_N \leq t_{N+1}$ are the switching times. We define $t_f = t_{N+1}$ as the final time. The pair (t_i, q_i) for $1 \leq i \leq N$ indicates that at time t_i the dynamics change from mode q_{i-1} to q_i. Thus, in the time interval $[t_i, t_{i+1})$, referred to as the i-th phase/operation, the state evolution is governed by the vector field f_{q_i}. As an illustration, an aircraft might be flying at constant speed mode

and then switch at t_1 to an accelerating/decelerating mode, due to a speed advisory.

The states and inputs must fulfill constraints for each mode $q \in Q$, compactly represented as

$$h_q(x(t), u(t)) \leq 0, \tag{2}$$

where in the above $h_q : \mathbb{R}^{n_x} \times \mathbb{R}^{n_u} \to \mathbb{R}^{n_h}$. These constraints are used to capture the flight envelope, operational constraints, collision avoidance constraints, or hazardous weather avoidance requirements.

The objective in optimization based trajectory planning is to find a feasible aircraft trajectory that minimizes a desired cost function such as fuel or time of flight. The hybrid optimal control problem is thus as follows: Given an initial condition $x(t_0)$, find a switching sequence σ and an input $u : [t_0, t_f] \to U$, that fulfill the dynamics (1), the constraints (2) and minimize a cost function $J(\sigma, u)$. That is, solve the following hybrid optimal control problem:

$$\begin{aligned} \min_{u,\sigma} \quad & J(u,\sigma) := \phi(x(t_f)) + \textstyle\sum_{i=0}^{N} \int_{t_i}^{t_{i+1}} L_{q_i}(x(t), u(t))dt \\ \text{s.t.} \quad & x(t_0) = x_0, \text{ and for } i \in [t_i, t_{i+1}],\ i = 0, \ldots, N, \\ & \dot{x}(t) = f_{q_i}(x(t), u(t)), \\ & h_{q_i}(x(t), u(t)) \leq 0. \end{aligned}$$

In the above, ϕ is referred to as the Mayer term, denoting a final cost, and the integral term in J is referred to as the Lagrange term, denoting a running cost. The final cost can be used to quantify the deviation from a desired final state, such as reaching a waypoint or a destination at a given time. The running cost can denote costs accumulated during the flight such as fuel consumption. The initial time t_0 is given while the final time t_f can be an optimization variable. For a well-defined problem, we assume that for all $q \in Q$ the functions f_q, h_q, ϕ, and L_q are Lipschitz continuous and differentiable.

The hybrid optimal control problem defined above is challenging for several reasons. First, the unknown number of mode switches, switching sequence and switching times result in a non-classical optimal control problem. Second, in realistic air traffic scenarios, multiple aircraft are involved and are coupled through collision avoidance constraints. Thus, the states, inputs and constraints are of high dimensions. Third, the dynamics and constraints are in general non-convex.

III. Solution Approach

To obtain a numerical solution to the formulated hybrid optimal control problem, our goal is to cast the problem as a nonlinear optimization program (NLP) and employ *off-the-shelf* NLP solvers. Our approach is summarized as follows. First, we introduce binary control functions for each mode to formulate the hybrid optimal control problem as a Mixed Integer Optimal Control Problem (MIOCP) [39]. Next, we relax the binary functions and include a penalty term on the relaxation, so that as the weight of the penalty term increases, the relaxed solution converges to a binary function. Finally, we apply a collocation discretization rule [40] to convert the continuous problem into an NLP. We now describe each step.

A. Formulation as MIOCP

Let $w_q : [t_0, t_f] \to \{0, 1\}$ denote a binary control function for each mode $q = 1, \ldots, n_q$. Let $\bar{f} : \mathbb{R}^{n_x} \times \mathbb{R}^{n_u} \times \{0,1\}^{n_q}$ be defined as $\bar{f} = \sum_{q=1}^{n_q} w_q f_q$. By adding the constraint $\sum_{q=1}^{n_q} w_q(t) = 1$, we ensure there is one active mode at each time t and so the dynamical system is well-defined. Similarly, define $\bar{h} = \sum_{q=1}^{n_q} w_q h_q$ and $\bar{L} = \sum_{q=1}^{n_q} w_q L_q$. Note that the switching sequence σ can be derived from $w(t) = [w_1(t), \ldots, w_{n_q}(t)]$, for $t \in [t_0, t_f]$. For example, suppose $w_i(t^-) = 1$ for $q = i$ and $w_j(t^+) = 1$ for $q = j$. Then, a switch from mode i to j occurs at time t.

The hybrid optimal control problem with the new control variables, dynamics, constraints, and cost function can be written as a Mixed Integer Optimal Control Problem (MIOCP):

$$\begin{aligned} \min_{u,w} \quad & J(u,w) = \phi(x(t_f)) + \textstyle\int_{t_0}^{t_f} \bar{L}(x(t), u(t), w(t))dt \\ \text{s.t.} \quad & x(t_0) = x_0, \text{ and } \forall t \in [t_0, t_f] \\ & \dot{x}(t) = \bar{f}(x(t), u(t), w(t)), \\ & \bar{h}(x(t), u(t), w(t)) \leq 0, \\ & w_q(t) \in \{0, 1\},\ q = 1, \ldots, n_q \\ & \textstyle\sum_{q=1}^{n_q} w_q(t) = 1. \end{aligned} \tag{MIOCP}$$

By discretizing the problem at this stage, one obtains a MINLP [27]. This results in n_q binary decision variables for each discretization step and thus, the problem becomes intractable for more than a few number of discrete modes.

B. Relaxation of binary constraints through a penalty term

First, we relax $w_q(t)$ by allowing it to belong to $[0, 1]$ instead of $\{0, 1\}$. Then, we define $\beta_q : [t_0, t_f] \to [-1, 1]$ for $q = 1, \ldots, n_q$, as a vector of auxiliary optimization variables, with $\beta_q(t) = 2w_q(t) - 1$. We define a penalty cost function $l : [0, 1] \to \mathbb{R}_{\geq 0}$, where l is strictly monotonically decreasing and $l(1) = 0$. With the relaxation and the penalty term, we formulate a classical optimal control problem as:

$$\begin{aligned} \min_{u,w,\beta} \quad & J(u,w,\beta) = \phi(x(t_f)) \\ & + \textstyle\int_{t_0}^{t_f} \left(\bar{L}(x(t), u(t), w(t)) + \alpha \sum_{q=1}^{n_q} l(|\beta_q(t)|) \right) dt \\ \text{s.t.} \quad & x(t_0) = x_0, \text{and } \forall t \in [0, t_f] \\ & \dot{x}(t) = \bar{f}(x(t), u(t), w(t)), \\ & \bar{h}(x(t), u(t), w(t)) \leq 0, \\ & \beta_q(t) \in [-1, 1],\ q = 1, \ldots, n_q, \\ & w_q(t) = \tfrac{1}{2}(1 - \beta_q(t)),\ q = 1, \ldots, n_q \\ & \textstyle\sum_{q=1}^{n_q} w_q(t) = 1. \end{aligned} \tag{R-MIOCP}$$

The control variables in the transformed problem are the input $u(t)$, the auxiliary inputs $\beta_q(t)$, the switching law $w_q(t)$ for $t \in [t_0, t_f]$, $q \in Q$ and the final time t_f. The constant α is a design parameter. While integer constraints are not explicitly added, the penalty term ensures that in practice for sufficiently large α, the optimized solution would approach $|\beta_q(t)| = 1$ and consequently, $w_q(t) \in \{0, 1\}$ for each $q \in Q$.

The relaxation of the binary variables in a hybrid optimal control problem has been proposed in the past, as briefly discussed in the introduction. For example, the approaches described in [35], [39] referred to as embedding or convexification, solve the relaxed problem. However, they do not include

any penalty term on the relaxed solution. Consequently, the optimized w in the relaxed problem will in general be non-binary, specially due to the constraints (2) of the optimal control problem considered here. As such, to obtain a feasible mode sequence, a projection of the relaxed solution to the binary variables is required. There are no unique or optimal ways of doing the projection. In addition, the continuous input u optimized for the relaxed solution may no longer be optimal or feasible. By using the penalty term, we aim to obtain an integer solution with increasing the penalty weight α. We note that the penalty method for MINLP has been studied in [41], [42]. Under additional assumptions on continuity of the objective and constraint functions, and appropriate choice of the penalty function the equivalence of the penalized problem and the original MINLP is shown.

C. Formulation as a Nonlinear Program

Problem (R-MIOCP) is a standard constrained optimal control problem. Due to non-convexities in dynamics and constraints, and high dimensions of states, inputs and constraints, we resort to numerical solution via discretization. With a time discretization of dynamics the optimal control problem can be converted to a nonlinear program (NLP for short). We use is the so-called Hermite-Simpson direct collocation method [40]. It has been widely used for solving optimal control problems in aircraft and aerospace applications due to its computational efficiency [43], [27].

Next, we show that as $\alpha \to \infty$, the optimal $w \in [0,1]^{n_s \times n_q}$ in the discretized problem converges to an integer solution $w \in \{0,1\}^{n_s \times n_q}$.

Consider the mixed integer nonlinear optimization problem below as an abstraction of the discretized optimal control problem with $n_s = 1$:

$$\begin{aligned} J^* = \min_{u,\beta} \quad & g(u,\beta) && (P)\\ \text{s.t.} \quad & b(u,\beta) \le 0 \\ & \beta \in \{-1,1\}^{n_q}. \end{aligned}$$

Here, b contains all discretized constraints in (R-MIOCP). The variable w and its constraints are implicitly accounted for by β. Let (u^*, β^*) denote the solution to this problem. We introduce a relaxation (convexification) of Problem (P):

$$\begin{aligned} J^r = \min_{u,\beta} \quad & g(u,\beta) && (P^r)\\ \text{s.t.} \quad & b(u,\beta) \le 0 && (3)\\ & \beta \in [-1,1]^{n_q}. && (4) \end{aligned}$$

Next, we introduce the penalized problem:

$$J^\alpha = \min_{u,\beta} \quad g(u,\beta) + \alpha \sum_{q=1}^{n_q} l(|\beta_q|) \qquad (P^\alpha)$$
$$\text{s.t. } (3), (4).$$

Furthermore, we let (u^r, β^r), (u^α, β^α) denote the solution to the relaxed and the penalized problem, respectively. We assume a unique optimizer for (P), (P^r), (P^α) exist.

Proposition 1. *Assume the penalty function $l : [0,1] \to \mathbb{R}_+$ is strictly monotonically decreasing, and $l(1) = 0$. Then, as $\alpha \to \infty$, $\beta^\alpha \to \beta^*$.*

Proof. If $\beta^r = \beta^*$ then $\beta^\alpha = \beta^*$ and the statement is shown. If $\beta^r \neq \beta^*$, then $J^r < J^*$ and thus there exists $C > 0$, such that $J^r + C = J^*$. Assume statement of the proposition does not hold. As such, let $(\alpha^n)_{n=0}^\infty \to \infty$ and $(\beta^n)_{n=0}^\infty$ be a sequence of corresponding optimizers, not converging to β^*. Then, $\exists \epsilon > 0$, and a subsequence $(\beta^k)_{k=0}^\infty$ such that $\|\beta^k - \beta^*\|_1 > \epsilon$. Since the penalty function l is strictly monotonically decreasing and $l(|\beta_q^*|) = 0$, we conclude $\sum_{q=1}^{n_q} l(|\beta_q^k|) \ge \delta > 0$ for some δ. Choose k large enough such that $\delta \alpha^k > C$. Notice that $g(u^r, \beta^r) \le g(u^\alpha, \beta^\alpha)$ since every feasible solution for (P^α) is also feasible for (P^r). Thus,

$$\begin{aligned} J^{\alpha_k} &= g(u^{\alpha_k}, \beta^{\alpha_k}) + \alpha^k \sum_{q=1}^{n_q} l(|\beta_q^{\alpha_k}|) \\ &> g(u^r, \beta^r) + C = J^* \\ &= g(u^*, \beta^*) + \alpha^k \sum_{q=1}^{n_q} l(|\beta_q^*|). \end{aligned}$$

The above contradicts that $(u^{\alpha_k}, \beta^{\alpha_k})$ is optimal for (P^α). □

The result can be readily extended to a sequence of binary variables $w(t_s) \in \{0,1\}^{n_s \times n_q}$, where n_s is the number of discretization points, with the penalty term enforced at every time instance. In addition, the proof can be extended to the case in which $l(1) = c_0$ for some constant $c_0 \in \mathbb{R}_+$ and is strictly monotonically decreasing as before. This type of penalty function is considered in the case study.

IV. Aircraft Fuel Optimization as a Hybrid Optimal Control Problem

A variable-mass 2 degree of freedom aircraft model with parameters based on BADA 3.6 [44] is considered. The equations of motion over a spherical Earth (considered as inertial reference) are:

$$\frac{d}{dt}\begin{bmatrix} V(t) \\ \chi(t) \\ \lambda(t) \\ \theta(t) \\ h_e(t) \\ m(t) \end{bmatrix} = \begin{bmatrix} \frac{T(t) - D(h_e(t), V(t), C_L(t)) - m(t)\cdot g \cdot \sin\gamma(t)}{m(t)} \\ \frac{L(h_e(t), V(t), C_L(t))\cdot \sin\mu(t)}{m(t)\cdot V(t)\cdot \cos\gamma(t)} \\ \frac{V(t)\cdot\cos\gamma(t)\cdot\cos\chi(t)}{R\cdot\cos\theta(t)} \\ \frac{V(t)\cdot\cos\gamma(t)\cdot\sin\chi(t)}{R} \\ 0 \\ -T(t)\cdot\eta(V(t)) \end{bmatrix}.$$

Given that the flight path angle is set to zero due to horizontal motion, one has the following algebraic equation:

$$0 = L(h_e(t), V(t), C_L(t)) \cdot \cos\mu(t) - m(t) \cdot g \cdot \cos\gamma(t)$$

The states are: the 2D position given by longitude λ and latitude θ, the true airspeed V, the heading angle χ, and the aircraft mass m. The altitude h_e is assumed to be constant and the flight path angle γ equal to zero. The bank angle μ, and the engine thrust T, are the control inputs, that is, $u(t) = (T(t), \mu(t))$. Lift $L = C_L S\hat{q}$ and drag $D = C_D S\hat{q}$ are the components of the aerodynamic force, with S being

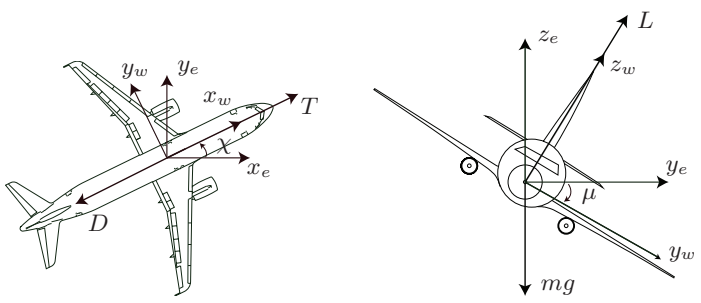

(a) Top view (b) Front view

Fig. 1. Aircraft state and forces. Subindices w and e refer to wind axis and local horizontal reference frames, respectively.

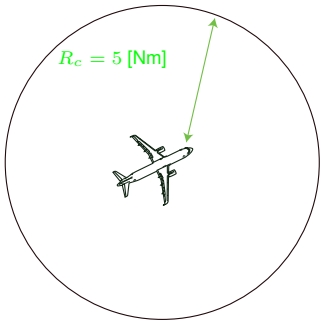

(a) Horizontal Separation

Fig. 2. Minimum required separation.

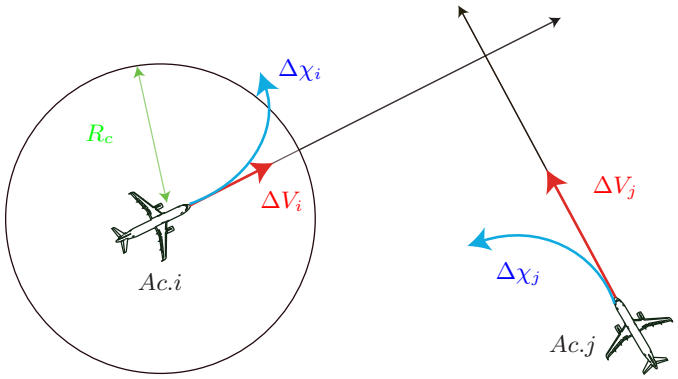

Fig. 3. Horizontal advisories. The black arrows indicate nominal aircraft heading and speed which leads to a conflict. The red arrows indicate the speed change advisory to avoid the conflict. The blue arrows indicate the heading change advisory to avoid the conflict. The later is referred to as vectoring in ATC terminology.

the reference wing surface area and $\hat{q} = \frac{1}{2}\rho V^2$ the dynamic pressure. Parabolic drag polar, $C_D = C_{D0} + KC_L^2$, and International Standard Atmosphere (ISA) are considered. The aircraft 2D position is approximated as $x_e = \lambda(R + h_e)\cos\theta$ and $y_e = (R + h_e)\theta$, with R being the radius of earth. η represents the specific fuel flow, which is a function of the airspeed. Aircraft state and forces are illustrated in Figure 1.

A. Constraints

1) Flight Envelope: Flight envelope constraints reflect the physical limits of the aircraft. This could be due to structural limitations, engine power, and aerodynamic characteristics. There may also be constraints due to operational limits, such as the maximum operational altitude. We use BADA performance limitation models and parameters [44] as follows:

$$\begin{aligned} &M(t) \le M_{M0}, && m_{min} \le m(t) \le m_{max}, \\ &\dot{V}(t) \le \bar{a}_l, && C_v V_s(t) \le V(t) \le V_{Mo}, \\ &\dot{\gamma}(t)V(t) \le \bar{a}_n, && 0 \le C_L(t) \le C_{L_{max}}, \\ &T_{min}(t) \le T(t) \le T_{max}(t), && \mu(t) \le \bar{\mu}. \end{aligned}$$

M_{M_0} denotes the maximum operating Mach number $M(t)$; $\bar{a}_n$ and $\bar{a}_l$ denote the maximum normal and longitudinal accelerations, respectively; $V_s(t)$ denotes the stall speed (C_v is a safety coefficient) and V_{M_0} denotes the maximum operating calibrated (CAS) airspeed; T_{min} and T_{max} denote the minimum and maximum available thrust, respectively. $\bar{\mu}$ denotes the maximum bank angle due to structural limitations.

2) Aircraft Conflict Constraint: Two aircraft flying at the same flight level are required to be separated by a distance of R_c nautical miles (typically 5 NM) in the horizontal plane, as shown in Fig. 2. Let (x^i, y^i) denote the Cartesian horizontal position of aircraft $i = 1, 2$ at time t. The conflict avoidance constraint is written as

$$\|(x^1, y^1) - (x^2, y^2)\|_2 \ge R_c.$$

Note that this constraint is not convex. The constraint needs to hold for each pair of aircraft involved in the conflict avoidance scenario at the beginning of the optimization horizon.

B. Objective Function

The objective function considered is minimization of total fuel consumption of all aircraft:

$$J = \sum_{i=1}^{n_a} \int_{t_0}^{t_f} \dot{m}_i(t)dt, \tag{5}$$

where n_a denotes the number of aircraft in the scenario, t_0 and t_f are the initial (typically fixed) and final time (fixed or free) of the scenario respectively. Note that to reflect the objective of the individual aircraft in fuel minimization, one can formulate a multi-objective optimization problem, with a vector of objective functions, $[J_1, \ldots, J_{n_a}]$, and search for the set of Pareto optimal solutions. The additive cost formulation above provides a single Pareto optimal solution in this set.

C. Flight Modes

In the en-route portion of flight, aircraft fly straight line segments connecting waypoints. To avoid conflict, the aircraft may be required to deviate from their nominal paths. In terms of ATC, these deviations are characterized by maneuvers which may consist of heading, speed, or altitude changes. Here, we restrict the maneuvers to horizontal advisories. In Figure 3 an example of such advisories for avoiding collision is sketched. We consider flight maneuvers as modes of the switched system. We characterize the horizontal maneuvers

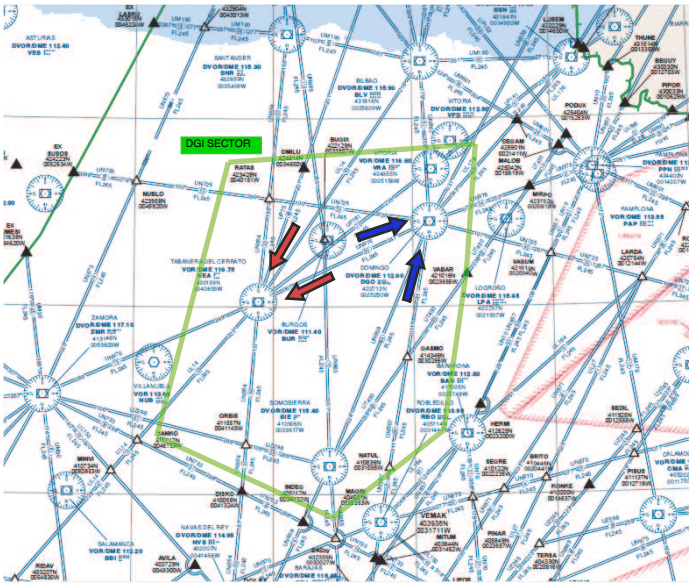

Fig. 4. Sketch of Sector DGI. Red arrows schematically represent conflicting flows at NEA VOR that occur at odd flight levels. Blue arrows schematically represent conflicting flows at DGO VOR that occur at even flight levels.

by two modes of *control speed* (mode 1) and *control heading* (mode 2). These maneuvers are routinely used in ATC since they are easily communicated to the pilots and are easily implemented by autopilots [18].

1) Control speed: The aircraft flies with variable speed but constant heading. The bank angle μ is set to zero. The engine thrust is the input, that is, $u(t) = T(t)$. This mode is an acceleration/deceleration mode; it gets activated when a speed advisory is given.

2) Control heading: The speed is held constant while the heading can change. The input is μ, that is, $u(t) = \mu(t)$. This mode is a turning mode (at constant airspeed); it gets activated a turn advisory is given.

V. Case Study

A realistic case study is presented to test the effectiveness of the approach. The chosen scenario is based on Sector Domingo (DGI) in Spain, illustrated in Figure 4[1]. First, we provide insight into the current operations of the DGI sector.

A. Current operations in Sector Domingo

The DGI sector is truly complex. This is because it gathers not only overflights, but also a large number of climbing or descending traffic, referred to as evolution traffic. The evolution traffic mostly correspond to LEMD, the Adolfo Suarez Madrid Barajas airport[2]. DGI is the sum of two sectors, DGL (lower) and DGU (upper). The divide between the lower and the upper sector is at FL345. During day operation and normal traffic, the sectors remain separate, and during night they are integrated into a single sector. Real declared capacities used by the Central Flow Management Unit (CFMU) are as follows: DGI: 40 aircraft per hour; DGU: 40 aircraft per hour; DGL 44 aircraft per hour.

1) Overflights: Overflights refer to aircraft cruising at constant flight level. There are two typical crossing points within DGI through which most of the overflight flows pass. The traffic is structured in such a way that flights going south-to-north and west-to-east fly at even flight levels, those going north-to-south and east-to-west fly at odd flight levels. Potential conflicts typically occur at DGO Very high frequency Omnidirectional Range (VOR) and NEA VOR. To resolve a conflict, ATCOs use a set of developed heuristics, a summary of which is given below for the most commonly occurring conflicts at DGO and NEA VORs.

Conflicts over DGO VOR occur at even levels between traffic flying south-to-north (via UN858 and UN867, that is SIE-DGO or NATUL-DGO) and traffic flying west-to-east (via UN725 and mostly UN976, that is RATAS-DGO or NEA-DGO). These conflicts could be resolved through heading, level changes or speed control maneuvers. However, most of these conflicts are normally resolved giving direct routings to the south-to-north flow, normally instructing them to fly directly towards BLV, LUSEM or ABRIX depending on the route. Since most of the NEA-DGO flow (west-to-east) is routed later via LATEK, and NEA-DGO-LATEK are almost aligned, giving direct routings to this flow would not be so useful for resolving conflicts since they hardly represent any change in the heading of the plane. Thus, the west-to-east flow remains typically untouched.

Conflicts over NEA VOR occur at odd levels between traffic flying north-to-south (via UN864, UP75 and UL14, that is SNR-NEA, OMILU-NEA or BLV-NEA) and traffic flying east-to-west (via UP181 and UN976, that is VRA-NEA or DGO-NEA). In analyzing a set of aircraft with this pattern, the first task is to identify any involved aircraft that is to arrive at LEMD (airport). In this case, the conflicts would be resolved by advising a vertical maneuver, which in turn results in forcing the arrival to start its descent slightly earlier than optimum (the arrival procedures at LEMD require flight over ORBIS at FL240 with North runway configuration or established at FL190 with South runway configuration). Once this has been addressed, the focus is on the remaining aircraft. For NEA conflicts, giving direct routings do not imply significant turns, and thus de-conflicting typically requires vectoring. Vectoring refers to forcing one or both aircraft involved in the conflict to change heading, as shown in Figure 3. A typical technique is to order the last aircraft in the crossing to turn towards the tail of the leading aircraft.

2) Evolution traffic: DGI has a high amount of evolution traffic. Most of this evolution traffic departs from LEMD and leaves the UIR via DELOG, BELEN, ABRIX or LUSEM, reaching normally their cruise level within DGI sector. If due to different circumstances (weight, winds, higher temperatures, etc.) the aircraft does not make an acceptable climb and there is a significant amount of overflight traffic, it is expected that the aircraft reaches its final level at the next collateral sector

[1]Notice that some of the acronyms for waypoints, VORs, etc. discussed here, might not appear in the figure or be hardly visible. The reader is encouraged to download the SPAIN's En-Route Upper Navigation Chart ENR 6.1-5 (http://www.enaire.es/csee/Satellite/navegacion-aerea/es/Page/1078418725020//Como-consultar-la-AIP.html) for more information on this end.

[2]All relevant International Civil Aviation Organization (ICAO) acronyms are included in the appendix.

(BLI or PAI). Arrivals to LEMD via ORBIS may also be an important source of attention for the DGL controller, specially when LEMD is operating under South Configuration (arrivals via ORBIS through runway 18R), since ORBIS would not only absorb traffic from NEA, but also traffic from ZMR. Other airports that deliver evolution traffic to this sector are LEBB, LEXJ, LEVT, LEVD, LELN and LEBG.

3) A real sample of traffic: In order to provide more insight to the real scenario, we have collected real flight data for DGU sector on September 4th 2014 between 0610Z and 0645Z[3], when LEMD was operating under South runway configuration. This is a typical weekday morning scenario. During these 35 minutes, and taking only into account the DGU sector (above FL345), a total of 15 aircraft entered the sector, with the data provided in Table I. There were only 3 departures from LEMD asking for a cruise Flight Level above FL345 (those climbing to even final levels), and there were no arrivals to LEMD through ORBIS. Even though only three aircraft were vectored to achieve valid separation distances, this does not imply low workload. Even if there are no conflicts, the workload can be high due to radio frequency congestion or due to flights that almost infringe the separation minima.

B. Problem set up

We consider a scenario with 7 aircraft, all modeled following BADA 3.6 [44], overflying sector DGI at FL 360, and within a time window of 10 minutes. Flight data have been selected according to Eurocontrol Demand Data Repository. In order to have a realistic number of conflicts to be resolved and therefore test the capabilities of the algorithm, the density of aircraft has been artificially increased. That is, the simulation scenario contains more conflicts than expected in reality for aircraft cruising at FL360. Notice that the real scenario is more complex than the case study presented in this paper because evolution traffic is not considered. Please refer to the previous section V-A3 for a qualitative measure of the complexity of the traffic in the sector.

Initial and final conditions of aircraft are provided in Table II. Aircraft (Ac.) 1, 2, 4, 5 overfly the sector eastwards, NEA to DGO. Ac. 3, Ac. 6, and Ac. 7 overfly the sector northwards: Ac. 3 follows SIE to DGO and Ac. 6 and 7 follow NATUL to DGO. According to the initial condition in Table II, assuming that the aircraft are to fly at constant airspeed and following the airways, there would be four unresolved conflicts around DGO VOR. These conflicts are between the pairs Ac. 6 - Ac. 3; Ac. 6 - Ac. 1; Ac. 3 - Ac.1; and Ac. 7 - Ac. 2. This number of conflicts is a fair representation of the current operational complexity in the DGI sector with the inclusion of evolution traffic and odd flight levels.

The problem of fuel optimal conflict avoidance is formulated as stated in Section II. We consider turn and speed advisories. In this case study, since there are two modes, a single binary control function $w(t) \in \{0,1\}$ for each aircraft is sufficient to capture the two modes. This binary control function is relaxed as described in Section III-B. The penalty of the relaxation in the objective function of Problem (R-MIOCP) is taken as

$$\alpha \sum_{q=1}^{n_q} (\beta_q(t))^d,$$

with $\alpha = -1$, $d = 2$. A discretization grid with a total of $n_s = 50$ sample points per aircraft have been used. The number of sample points has been selected by accounting for the capabilities of the algorithm for conflict detection and the computational time. [4]

C. Numerical results

The resulting large-scale NLP problem, with 4416 variables, 3208 equality constraints, and 4172 inequality constraints, has been solved using IPOPT [45]. Due to non-convexities, the solution obtained can only be claimed as locally optimal. The total computational time on a Mac OS X 2.56 GHz laptop with 4 GB RAM was 474 [s]. Important issues to take into consideration in order to reduce computational time are threefold: to properly scale the equations, to properly order the system equations so that the resulting Jacobian and Hessian matrices are sparse, and to initialize the NLP with a sufficiently good initial guess. The latter is specially critical. A two step process has been implemented to obtain a suitable initial guess: a) the free routing problem is solved (61 sec. computational time); b) its solution is post-processed and used as initial guess for both state and control variables, whereas the decision variables $\beta(t)$ are set to -1. The problem takes 413 to be solved. All in all, as already mentioned the whole process takes 474 sec. to be solved.

The number of switchings (number of advisories), the corresponding sequence of active modes (sequence of advisories), and the control inputs for each mode are provided by the solution to the NLP. Table III shows the fuel consumptions, flight times, and number of advisories for the different aircraft. Notice that all conflicts have been eliminated. The number of advisories results from the number of switchings of the binary control functions $w(t)$, which are illustrated in Figure 5. Here, $w(t) = 0$ corresponds to a control speed mode and $w(t) = 1$ corresponds to a control heading mode. Thus, switching between $w(t^*) = 0$ and $w(t^*) = 1$ at time t^* corresponds to a turn advisory and the switching between $w(t^*) = 1$ and $w(t^*) = 0$ at time t^* corresponds to a speed advisory.

Airspeed, heading angle, bank angle, and thrust profiles are depicted in Figure 6. The resulting optimal paths are illustrated in Figure 8. From these figures we observe the following characteristics of the solution. The optimal solution for Ac. 2, Ac. 4, Ac. 5, and Ac. 7 first slightly modifies the heading angle (by means of control heading mode) to head the aircraft towards the exit waypoints and then to maintain course and proceed at the optimal speed profile (by means of control speed mode). This behavior is very close to optimal performance characterized by orthodormic (or great circle) routing and

[3]Z refers to Coordinated Universal Time (Zulu).

[4]The same problem has been solved with increasing number of samples per aircraft, i.e., 75, 100, 150, obtaining equivalent solutions at a significative higher computational times.

TABLE I
AN EXAMPLE OF AIR TRAFFIC DATA FROM REAL OPERATIONS IN DGU SECTOR

Aircraft	Even FL	Route	Aircraft	Odd FL	Route
B738	380 established	NATUL-DGO-LUSEM	A320	370 established	DGO-NEA-ZMR
A320	360 established	NATUL-DGO-LUSEM	A319	390 established	DGO-NEA-ZMR
B738	climbing to 380	NATUL-DGO-LUSEM	A320	390 established	VRA-NEA-ZANKO
E190	climbing to 360	NATUL-DGO-LUSEM	A321	350 established	VRA-NEA-ZANKO
A332	400 established	RATAS-DGO-VASUM	A319	390 established	RATAS-NEA-ORBIS
B738	climbing to 380	NATUL-DGO-LUSEM	B752	370 established	RATAS-NEA-ORBIS
A333	400 established	NEA-DGO-LATEK	A320	350 established	DGO-NEA-ZMR
B738	360 established	SIE-BUGIX-DELOG			

TABLE II
BOUNDARY VALUES OF THE AIRCRAFT FLYING THROUGH SECTOR DGI

Aircraft	ORI-DEST	Ac. Type	Sector entry values						Sector exit values	
			t [s]	m [kg]	V [kt]	λ_e°	θ_e°	Radial (measured from DGO VOR)	λ_e°	θ_e°
Ac. 1	LIS-FRA	A320	0	$0.8 \cdot m_{ref}$	460	-4.53	41.83	R247	-2.60	42.65
Ac. 2	OPO-MRS	B737-800	120	$0.8 \cdot m_{ref}$	420	-4.53	41.83	R247	-2.60	42.48
Ac. 3	ACE-HAN	B737-800	0	$0.8 \cdot m_{ref}$	440	-3.72	40.91	R204	-2.60	42.84
Ac. 4	SEA-FRA	A340	240	$0.8 \cdot m_{ref}$	480	-4.53	41.83	R247	-2.60	42.65
Ac. 5	OPO-GVA	A319	360	$0.8 \cdot m_{ref}$	460	-4.53	41.83	R247	-2.60	42.48
Ac. 6	FUE-CGN	A319	0	$0.8 \cdot m_{ref}$	430	-3.17	41.14	R191	-2.86	42.81
Ac. 7	TFE-BRU	B737-700	120	$0.8 \cdot m_{ref}$	430	-3.17	41.14	R191	-2.86	42.81

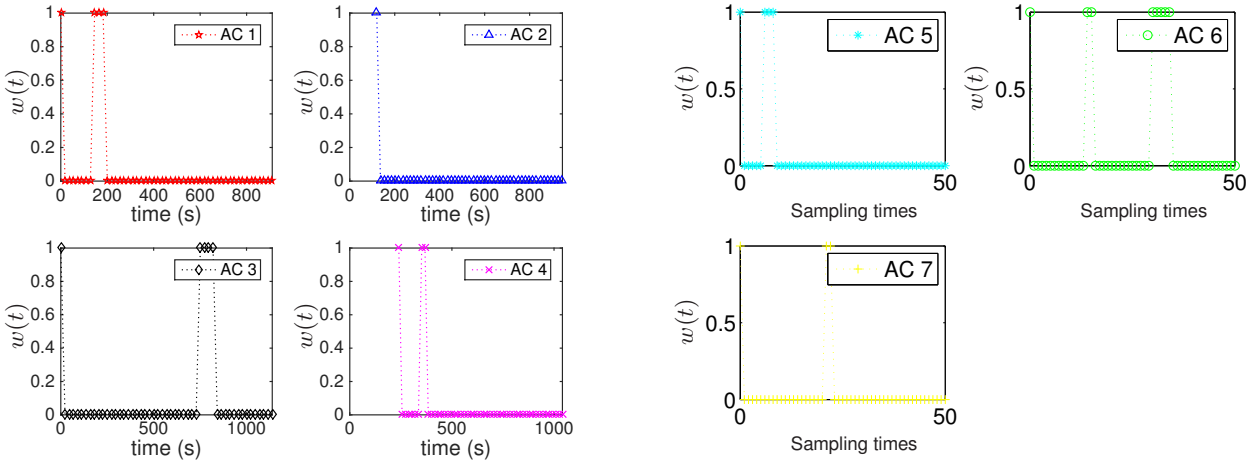

(a) $w(t)$ in Aircraft 1, 2, 3, 4

(b) $w(t)$ in Aircraft 5, 6, 7

Fig. 5. Binary control functions $w(t)$ as a function of time. Here, $w = 1$ represent a control speed mode.

optimal speed profile. Nevertheless this solution strategy does not apply to Ac.1, Ac. 3, and Ac. 6, because such a strategy would automatically imply conflicts. For both Ac. 3, and Ac. 6 a turn advisory is instructed near DGO (see 6(c)). Also these two aircraft, together with Ac.1, present speed advisories (see 6(a)). By these maneuvers, potential conflicts between Ac. 6 - Ac. 3; Ac. 6 - Ac. 1; Ac. 3 - Ac.1 have been avoided. Conflict between Ac. 7 - Ac. 2 can be avoided by simply flying the optimal profile (instead of following airways and constant speed procedures).

To illustrate the potential benefits in terms of fuel consumption, we compare the obtained results with two different operational concepts over the above exposed scenario:

1) A minimum fuel benchmark case in which aircraft are allowed to fly under free routing operational concept (labeled as *free routing*).
2) A case resembling the current operational concept, that is, aircraft flying constant speed and following airways and waypoints (labeled as *current paradigm*)

TABLE III
NUMERICAL RESULTS

	Fuel consum. [kg]	Time [s]	num. advisories
Ac. 1	390.2	903	2
Ac. 2	413.8	945.8	1
Ac. 3	563.8	1104.8	2
Ac. 4	941.0	1041.0	2
Ac. 5	340.7	1302.4	2
Ac. 6	390.6	1014.1	3
Ac. 7	416.7	1003.1	2

In both operational concepts aircraft conflicts are not considered, i.e., solutions provided in both cases include unresolved conflicts. Optimal paths for the free routing and current operational concept are available in Figure 8 within Appendix A.

Table IV, which has been also brought back to Appendix A

for the sake of clarity, shows fuel consumption, flight times, and conflicts. The current paradigm presents a relatively high overall fuel consumption. Moreover, without ATCO stepping in, four unresolved conflicts are encountered. As expected, the free routing scenario presents the least overall consumption. However, three of the conflicts remain unresolved. These conflicts are between the pairs Ac. 3 - Ac. 6, Ac. 1 - Ac. 6, Ac. 1 - Ac. 3. On the contrary, the proposed CA algorithm (which in essence actuates on Ac. 1, Ac. 3, and Ac. 6) is capable of resolving all conflicts with an overall fuel consumption that is close to the optimal free routing benchmark. A total of 450 [kg] (around 15%) fuel could potentially be saved. Nevertheless, this saving could be at the cost of increased travel time compared to the current paradigm.

D. Discussion on the results

1) Expected ATCO behavior in the given scenario: We can only speculate on how an ATCO would have acted given the proposed scenario. It is important to note that each human may act differently. The following comments only represent the views of the authors.

a) ATCO behavior under current operational concept: For the proposed complex scenario under the current operational concept, as shown in Figure 8(b), and given current technology, we think that an ATCO would have focused on reaching a safe solution by either vectoring or giving free routing advises to some of the aircraft to achieve the required separation. If the complexity of the scenario were too high and the ATCO felt overwhelmed, he would have ordered one of the conflicting aircraft to change its flight level, possibly leading to a less efficient solution. Even though speed resolutions might apply, ATCO tend to not use them in complex scenarios because speed is highly uncertain, particularly due to wind and measurement inaccuracies, and thus trajectories of the involved aircraft are more difficult to predict.

b) ATCO behavior under free-routing operational concept: For the *free routing* operational concept shown in Figure 8(a), it is hard to imagine how an ATCO would have reacted since all ATCOs currently know and foresee the behavior of the aircraft within their domain. It seems unacceptable for an ATCO not to know in advance how an aircraft is going to react, in terms of changes of heading and speed. An environment in which the uncertainty of aircraft motion is large would be strongly stressful and thus unsafe for the human in the loop.

c) ATCO behavior within the operational concept arising from proposed CA algorithm: The future air navigation system to be built around SESAR will provide its users access to datalink communications, ADS-B, Mode-S Radar and other evolved communication and surveillance systems. Aircraft will be able to upload its preferred business trajectory via datalink (previously optimized according to its business interests). Such trajectory would have been de-conflicted strategically and/or pre-tactically using algorithms similar to the ones presented in this paper. ATCO would have a supervisory role, approving or rejecting the proposed aircraft intents. The most important contribution of the solution provided by the CA algorithm is that aircraft behaviors are predictable. In other words, compared to free routing solutions, CA algorithm solution are more likely to be trusted and accepted by humans. In this setup, ATCO can take control in the case in which they deem the proposed trajectories unsafe.

2) Limiting assumptions: The presented approach include assumptions that limit its application and motivate future work:

(a) The model does not deal with evolution traffic, or vertical level changes for conflict resolution. A flight level change may be more fuel efficient and safer than heading and speed advisories in certain circumstances.
(b) The model is not taking into account traffic in adjacent sectors. Depending on the nearby sector traffic the solution may be unacceptable by collateral sectors, causing a *domino* effect and perturbing the flows of traffic within the network.
(c) Currently, the nominal minimum separation value is 5 nm. However, when the leading aircraft is heavy and the preceding one is light, due to wake vortex the minimum separation is 6 nm. This was not included in the model.
(d) The solution did not result in equal distribution of fuel savings among the aircraft. Airlines may require a fair solution. Also, there may be aircraft with priorities in terms of not modifying their trajectories.
(e) Wind or uncertainties that may affect the predictability of the trajectories have not been considered.

Most of these items could be accommodated with the proposed hybrid optimal control algorithm. However, this will come at the cost of numerical tractability of the problem. Item (a) could be considered by introducing 3D aircraft dynamics, together with vertical mode changes and FL structure. Item (b) could be tackled by imposing required/control time of arrivals (RTA/CTA) at exit waypoints. Item (c) can simply be addressed by defining minimal separation requirements based on aircraft weights. Item (d) has to do with weighting the cost of fuel for different companies, which in turn means establishing priorities in the use of airspace. Regarding item (e), whereas deterministic wind forecasts could be included in the problem, the most challenging issue is to tackle the uncertainties introduced by the atmosphere (wind, temperature, hazards). An elegant way to proceed would be to recast the problem as a stochastic hybrid optimal control problem. Another approach is to artificially increase the minimum separation constraints (for instance, to 6-7 NM) to account for possible deviations from the computed trajectories with a buffer. The latter has been tested with increasing separation minima of 5.5, 6, 6.5, and 7 NM with successful results.

We also note that the simultaneous use of both modes (speed and heading change, i.e., free routing) is a strategy that is almost exclusive in approach (arrival aircraft) control. Its application to en-route control will increase efficiency of the overall system. It can also be accommodated in our optimal control framework, as illustrated in the free-routing solution. The key factor for success of this strategy relies on implementation methods in which the ATCOs do not see a complexity or workload increase.

3) Limitations for implementation in real life:

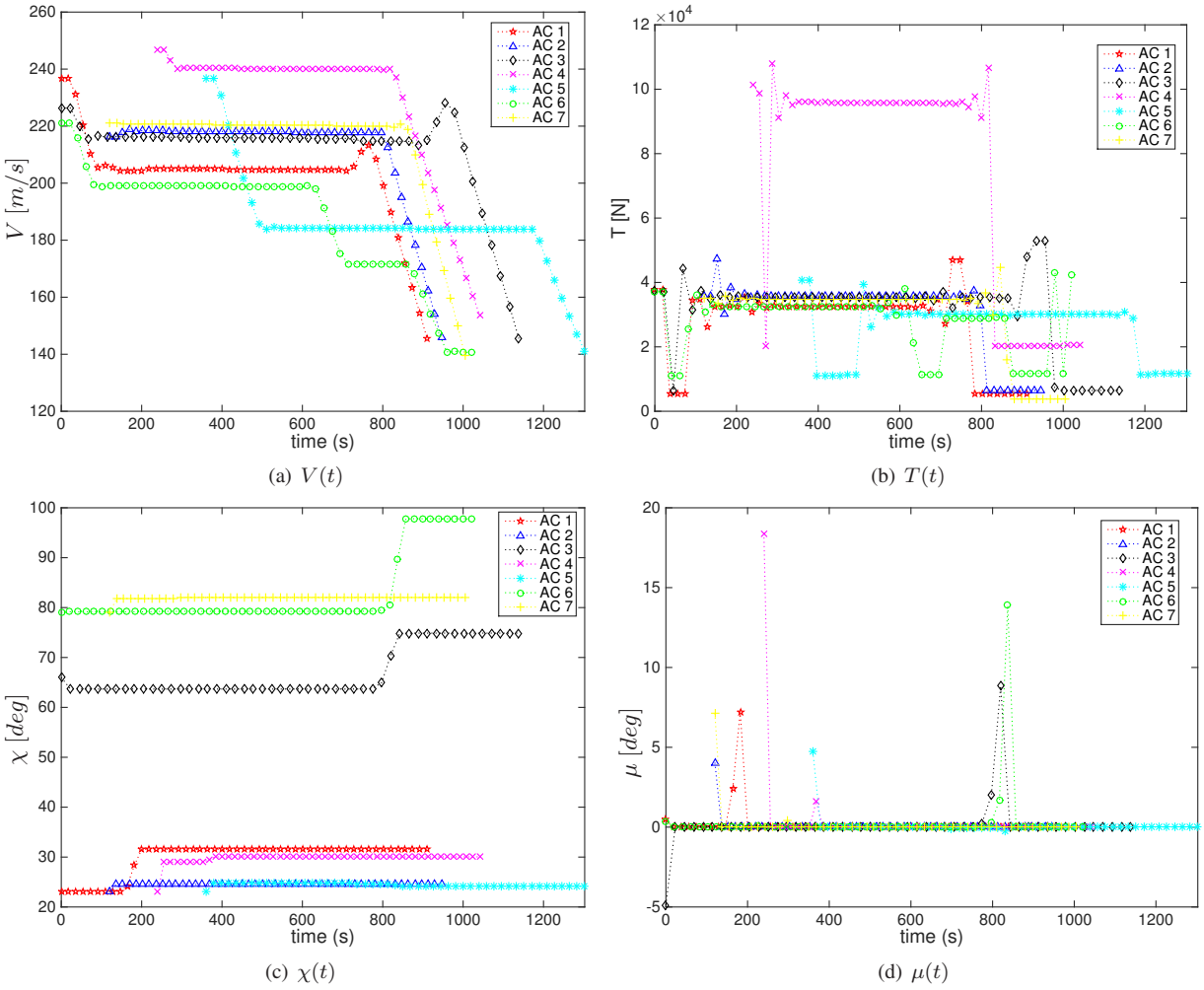

(a) $V(t)$ (b) $T(t)$

(c) $\chi(t)$ (d) $\mu(t)$

Fig. 6. Evolution of state and control variables over time

(a) With current equipment, the aircraft cannot turn by one magnetic degree resolution, that is, a pilot cannot select a heading of 15.7°, decimally, but only 16°. This reduces the accuracy of the solution. Current procedures applied by ATCOs force aircraft to turn by increments of 5 degrees, that is, normal vectoring requires turns of 5, 10, 15 or even 20 degrees; a turn of 17 degrees, for instance, is currently not used since there is no knowledge nor certainty to resolve conflicts with such accuracy.

(b) The computational time (474 seconds for the given case-study) exceeds the required anticipation and real-time decision making process needed. Typically an ATCO does not think about how to solve a conflict for more than 10 to 15 seconds before applying it.

(c) The simulation produced 14 advisories for 7 aircraft, an average of 2 advisories per aircraft only within the DGI Sector. This is a large number compared to current available workload capacity and performance. Thus, the output of the algorithm, for the proposed scenario would not be applicable in real life with the current human support. The results could be implementable if the ATCO only approves and monitors the proposed solution without instructing the 14 different advisories.

(d) Within the work of an ATC, it is important not only to monitor the current state of the system, but also to be able to predict the evolution of the system fairly well. In order to trust the solution, ATCO would feel comfortable only if it can be shown that the uncertainty in the future evolution of the solution is negligible and aircraft are easily trackable by the interface that ATCOs use.

To summarize, the algorithm should be compatible with aircraft equipment, faster in terms of computation time and transparent for an ATCO. In this case, the role of ATCO would only be to select the conflicting aircraft and approve a separation using these algorithms, making sure that there are no other possible negative consequences in terms of safety.

Some of these limitations (such as computational time and/or excessive number of advisories) are subject of further research. The remaining would be partially addressed thanks to SESAR through better equipment and advanced human decision support tools.

4) On the alignment of the proposed algorithm with SESAR: As mentioned in the introduction, the European ATM (also United States, Japan, and Australia's ones) is undergoing a tremendous change to cope with future needs in four key performance areas of safety, capacity, environment and cost-

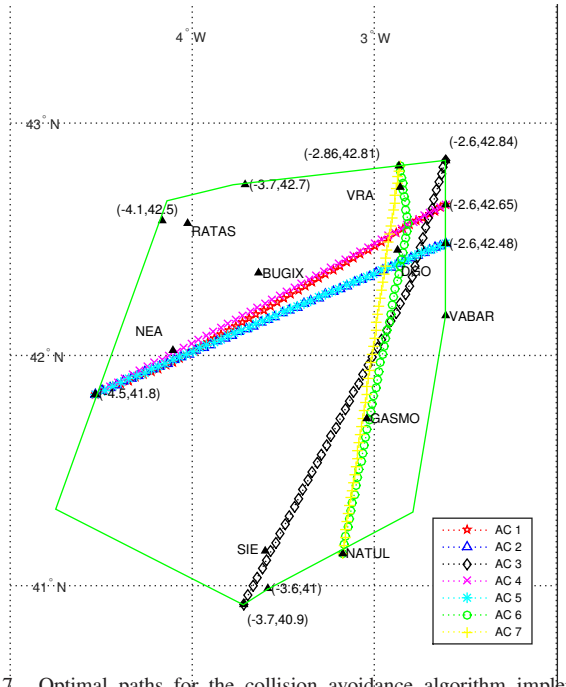

Fig. 7. Optimal paths for the collision avoidance algorithm implemented in this paper. The triangles represent waypoints, the bounded region is a geometric representation of the DGI sector.

efficiency. To meet these performance objectives, SESAR Master Plan [1] proposes roadmaps of essential operational changes shifting from the current operational concept (based on the airspace structure) to the so-called trajectory-based operational concept (medium term) and further to the so-called performance-based operational concept (long term).

To address this ambitious roadmap, SESAR has identified six features of business areas for research and innovation. One of these areas is the so-called conflict management and automation, which aims at substantially reducing controller task load per flight through a significant enhancement of integrated automation support, while simultaneously meeting the safety and environmental goals of SESAR. Human operators will remain at the core of the system (overall system managers and supervisories) using automated systems with the required degree of integrity and redundancy. Humans will be fully adapted to SESAR future trajectory management systems and new separation modes, thus ensuring their effectiveness as a last safety layer against the risk of collision and other hazards.

Based on the results and discussion above, the proposed conflict avoidance algorithm is therefore aligned with SESAR roadmap. It aims at contributing to improvements in the key performance areas, reducing fuel consumption and CO_2 emissions while ensuring safety through the development of trajectory/performance based algorithms. It also maintains the human in the loop by deploying conflict-free trajectories composed of operating modes. Thus, the results are more tractable by humans than fully automated free-routing concepts.

VI. Conclusions

We formulated fuel optimal conflict free aircraft trajectory planning as a hybrid optimal control problem. This formulation allowed for inclusion of 3 DoF aircraft dynamic model and conflict resolution maneuvers that are consistent with ATC procedures. We developed an algorithm for solving the hybrid optimal control problem through transforming it to a nonlinear program. Our approach was illustrated with a case study with accurate civilian aircraft model and realistic number of aircraft. In the case study, we considered an abstraction of real traffic in which only overflights, but realistic number of aircraft and conflicts, were considered. For this formulation, we derived fuel efficient advisories in a cognitive friendly manner. While there are several limitations in terms of realistic implementation, the case study presents a promising approach towards the development of human decision support tools that would aid ATCOs to ensure minimum separation and at the same time reduce fuel consumption and anthropogenic CO_2 emissions. Future steps include addressing the limitations discussed in Section V-D.

Appendix A
Optimal Paths

Times, fuel consumption and number of conflicts for the three operational concepts studied in this paper can be checked in Table IV. Optimal paths for the free routing operational concept and current operational concept are available in Figure 8.

Appendix B
ICAO Acronyms

This appendix contains the International Civil Aviation Organization (ICAO) acronyms used throughout the text:

LMED	=	Adolfo Suarez Madrid Barajas Airport
LEBB	=	Bilbao Airport
LEXJ	=	Santander Airport
LEVT	=	Vitoria Airport
LEVD	=	Valladolid Airport
LELN	=	Leon Airport
LEBG	=	Burgos Airport
DGI	=	ATC en-route sector Domingo
DGU	=	ATC en-route sector Upper Domingo
DGL	=	ATC en-route sector Lower Domingo
DGO	=	Navaid associated to DGO VOR
NEA	=	Navaid associated to NEA VOR
BLV	=	Navaid associated to BLV VOR
SNR	=	Navaid associated to SNR VOR
VRA	=	Navaid associated to VRA VOR
SIE	=	Navaid associated to SIE VOR
Waypoints	=	RATAS,NATUL,LUSEM,ABRIX,OMILU ORBIS,BUGIX,GASMO,DELOG,BELEN
Airways	=	UN858,UN867,UN725,UN976,UN864 UP75,UL14,UP181,UN976

References

[1] SESAR Joint Undertaking, "SESAR Master Plan, 2nd Edition," SESAR, Tech. Rep., 2012. [Online] Availble: http://ec.europa.eu/transport/modes/air/sesar.

TABLE IV
COMPARISON OF FUEL CONSUMPTION AND TIME OF FLIGHT FOR DIFFERENT TRAJECTORY PLANNING CONCEPTS

	free routing			CA Algorithm			current paradigm		
	Time	**Consum.**	**Conflicts**	**Time**	**Consum.**	**Conflicts**	**Time**	**Consum.**	**Conflicts**
Ac. 1	861.5	386.9	Ac. 3, Ac. 6	903	390.2	-	780.7	443.8	Ac. 6, Ac. 3
Ac. 2	946	413.8	-	945.8	413.8	-	933.7	448.4	7
Ac. 3	1095	561.1	Ac. 6	1104.8	563.8	-	1031.9	597.5	Ac. 6, Ac. 1
Ac. 4	1041	940.7	-	1040	941.0	-	988.3	1109.7	-
Ac. 5	1311	339.2	-	1302.4	340.7	-	1102.9	426.3	-
Ac. 6	1034	381	Ac. 1, Ac. 3	1014.1	390.6	-	855.2	438.3	Ac. 1, Ac.3
Ac. 7	1003	416.7	-	1003.1	416.7	-	975.2	452.7	Ac. 2
$\sum$ Total	7291	3343.94	3	7314.2	3456.8	0	6668	3916.7	4

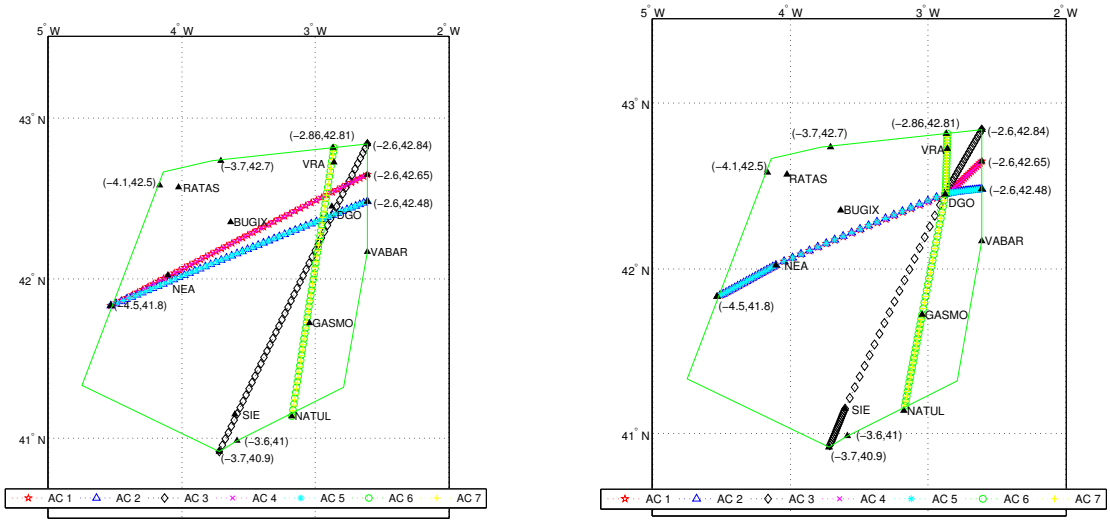

(a) Optimal paths for a free routing operational concept (trajectories are not deconflicted)

(b) Optimal paths for the current operational concept (trajectories are not deconflicted)

Fig. 8. Optimal paths. The triangles represent waypoints, the bounded region is a geometric representation of the DGI sector.

[2] Joint Planning and Development Office, "NEXTGEN. Concept of Operations for the Next Generation Air Transportation System, Version 2.0," 2007. [Online]. Available: http://www.jpdo.gov/library/nextgen_v2.0.pdf

[3] J. K. Kuchar and L. C. Yang, "A review of conflict detection and resolution modeling methods," *IEEE Transactions on Intelligent Transportation Systems*, vol. 1, no. 4, pp. 179–189, December 2000.

[4] F. J. Martín-Campo, "The collision avoidance problem: methods and algorithms," Ph.D. dissertation, Universidad Rey Juan Carlos, 2010.

[5] G. Chaloulos, J. Lygeros, and I. Roussos, "ifly deliverable d5. 1 comparative study of conflict resolution methods," *Thematic Priority*, vol. 1, no. 1.4.

[6] L. Pallottino, E. Feron, and A. Bicchi, "Conflict resolution problems for air traffic management systems solved with mixed integer programming," *IEEE Transactions on Intelligent Transportation Systems*, vol. 3, no. 1, pp. 3–11, 2002.

[7] A. E. Vela, S. Solak, J. Clarke, W. E. Singhose, E. R. Barnes, and E. L. Johnson, "Near real-time fuel-optimal en route conflict resolution," *Intelligent Transportation Systems, IEEE Transactions on*, vol. 11, no. 4, pp. 826–837, 2010.

[8] A. Alonso-Ayuso, L. Escudero, and F. Martín-Campo, "Collision avoidance in air traffic management: A mixed-integer linear optimization approach," *IEEE Transactions on Intelligent Transportation Systems*, no. 99, pp. 1–11, 2011.

[9] S. Cafieri and N. Durand, "Aircraft deconfliction with speed regulation: new models from mixed-integer optimization," *Journal of Global Optimization*, vol. 58, no. 4, pp. 613–629, 2014.

[10] G. Chaloulos, P. Hokayem, and J. Lygeros, "Hierarchical control with prioritized mpc for conflict resolution in air traffic control?" in *Proceedings of the 18th IFAC World Congress*, 2011, pp. 1564–1569.

[11] M. A. Christodoulou and S. G. Kodaxakis, "Automatic commercial aircraft-collision avoidance in free flight: the three-dimensional problem," *Intelligent Transportation Systems, IEEE Transactions on*, vol. 7, no. 2, pp. 242–249, 2006.

[12] A. Alonso-Ayuso, L. F. Escudero, and F. J. Martín-Campo, "A mixed 0–1 nonlinear optimization model and algorithmic approach for the collision avoidance in atm: Velocity changes through a time horizon," *Computers & Operations Research*, vol. 39, no. 12, pp. 3136–3146, 2012.

[13] J. Omer and J.-L. Farges, "Hybridization of nonlinear and mixed-integer linear programming for aircraft separation with trajectory recovery," *Intelligent Transportation Systems, IEEE Transactions on*, vol. 14, no. 3, pp. 1218–1230, 2013.

[14] T. Tarnopolskaya and N. Fulton, "Optimal cooperative collision avoidance strategy for coplanar encounter: Merzs solution revisited," *Journal of optimization theory and applications*, vol. 140, no. 2, pp. 355–375, 2009.

[15] X.-B. Hu, S.-F. Wu, and J. Jiang, "On-line free-flight path optimization based on improved genetic algorithms," *Engineering Applications of Artificial Intelligence*, vol. 17, no. 8, pp. 897–907, 2004.

[16] J. Betts and I. Kolmanovsky, "Practical methods for optimal control using nonlinear programming," *Applied Mechanics Reviews*, vol. 55, p. B68, 2002.

[17] R. Menon, G. Sweriduk, and B. Sridhar, "Optimal strategies for free-flight air traffic conflict resolution," *Journal of Guidance Control and Dynamics*, vol. 22, pp. 202–211, 1999.

[18] C. Tomlin, G. Pappas, and S. Sastry, "Conflict resolution for air traffic

management: A study in multiagent hybrid systems," *IEEE Transactions on Automatic Control*, vol. 43, no. 4, pp. 509–521, 2002.
[19] W. Glover and J. Lygeros, "A stochastic hybrid model for air traffic control simulation," in *Hybrid Systems: Computation and Control*, ser. Lecture Notes in Computer Science, R. Alur and G. J. Pappas, Eds., 2004, vol. 2993, pp. 372–386.
[20] I. Ross and C. D'Souza, "Hybrid optimal control framework for mission planning," *Journal of Guidance, Control and Dynamics*, vol. 28, no. 4, p. 686, 2005.
[21] M. Soler, D. Zapata, A. Olivares, and E. Staffetti, "Framework for Aircraft Trajectory Planning Towards an Efficient Air Traffic Management," *Journal of Aircraft*, vol. 49, no. 1, pp. 341–348, Jan-Feb 2012.
[22] M. Soler, A. Olivares, and E. Staffetti, "Multiphase optimal control framework for commercial aircraft four dimensional flight planning problems." *Journal of Aircraft*, 2014, In press (doi: 10.2514/1.C032697).
[23] S. Sager, "Numerical methods for mixed-integer optimal control problems," Ph.D. dissertation, Universität Heidelberg, 2006.
[24] P. Bonami, A. Olivares, M. Soler, and E. Staffetti, "Multiphase mixed-integer optimal control approach to aircraft trajectory optimization," *Journal of Guidance, Control, and Dynamics*, vol. 36, no. 5, pp. 1267–1277, 2013.
[25] I. Grossmann, "Review of nonlinear mixed-integer and disjunctive programming techniques," *Optimization and Engineering*, vol. 3, no. 3, pp. 227–252, 2002.
[26] P. Bonami, L. Biegler, A. Conn, G. Cornuéjols, I. Grossmann, C. Laird, J. Lee, A. Lodi, F. Margot, N. Sawaya *et al.*, "An algorithmic framework for convex mixed integer nonlinear programs," *Discrete Optimization*, vol. 5, no. 2, pp. 186–204, 2008.
[27] M. Soler, M. Kamgarpour, C. Tomlin, and E. Staffetti, "Multiphase mixed-integer optimal control framework for aircraft conflict avoidance," in *IEEE Conference on Decision and Control*, 2012, pp. 1740–1745.
[28] A. Bemporad and M. Morari, "Control of systems integrating logic, dynamics, and constraints," *Automatica*, vol. 35, pp. 407–428, 1999.
[29] M. S. Branicky and S. K. Mitter, "Algorithms for optimal hybrid control," in *IEEE Conference on Decision and Control*, Dec. 1995, pp. 2661– 2666.
[30] M. Shaikh and P. Caines, "On the hybrid optimal control problem: Theory and algorithms," *IEEE Transactions on Automatic Control*, vol. 52, no. 9, pp. 1587–1603, 2007.
[31] M. Alamir and S.-A. Attia, "An efficient algorithm to solve optimal control problems for nonlinear switched hybrid systems," in *Proceedings of IFAC symposium*, Sep. 2004, pp. 417–422.
[32] H. Sussmann, "A maximum principle for hybrid optimal control problems," in *IEEE Conference on Decision and Control*, vol. 1, 1999, pp. 425–430.
[33] X. Xu and P. Antsaklis, "Results and perspectives on computational methods for optimal control of switched systems," in *Hybrid Systems: Computation and Control*, ser. Lecture Notes in Computer Science, O. Maler and A. Pnueli, Eds. Springer, 2003, vol. 2623, pp. 540–555.
[34] H. González, R. Vasudevan, M. Kamgarpour, S. S. Sastry, R. Bajcsy, and C. J. Tomlin, "A descent algorithm for the optimal control of constrained nonlinear switched dynamical systems," in *Hybrid Systems: Computation and Control*, ser. Lecture Notes in Computer Science, K. H. Johansson and W. Yi, Eds., 2010, pp. 51–60.
[35] S. Bengea and R. DeCarlo, "Optimal control of switching systems," *Automatica*, vol. 41, no. 1, pp. 11 – 27, 2005.
[36] R. Meyer, M. Žefran, and R. A. DeCarlo, "A comparison of the embedding method to multi-parametric programming, mixed-integer programming, gradient-descent, and hybrid minimum principle based methods," *arXiv preprint arXiv:1203.3341*, 2012.
[37] S. Sager, H. G. Bock, and G. Reinelt, "Direct methods with maximal lower bound for mixed-integer optimal control problems," *Mathematical Programming*, vol. 118, no. 1, pp. 109–149, 2009.
[38] M. Soler, M. Kamgarpour, and J. Lygeros, "A numerical framework and benchmark case study for multi-modal fuel efficient aircraft conflict avoidance," in *6th International Conference on Research in Air Transportation (ICRAT)*, 2014.
[39] S. Sager, G. Reinelt, and H. Bock, "Direct Methods With Maximal Lower Bound for Mixed-Integer Optimal Control Problems," *Mathematical Programming*, vol. 118, no. 1, pp. 109–149, 2009. [Online]. Available: http://mathopt.de/PUBLICATIONS/Sager2009.pdf
[40] C. R. Hargraves and S. W. Paris, "Direct trajectory optimization using nonlinear programming and collocation," *Journal of Guidance, Control, and Dynamics*, vol. 10, no. 4, pp. 338–342, 1987.
[41] R. A. Shandiz and N. Mahdavi-Amiri, "An exact penalty approach for mixed integer nonlinear programming problems," *American Journal of Operations Research*, vol. 1, p. 185, 2011.
[42] S. Lucidi and F. Rinaldi, "Exact penalty functions for nonlinear integer programming problems," *Journal of optimization theory and applications*, vol. 145, no. 3, pp. 479–488, 2010.
[43] J. T. Betts, *Practical Methods for Optimal Control Using Nonlinear Programming*. SIAM, 2001.
[44] A. Nuic, *User Manual for the Base of Aircraft Data (BADA) Revision 3.6*, Eurocontrol Experimental Center, 2005.
[45] A. Wächter and L. Biegler, "On the implementation of an interior-point filter line-search algorithm for large-scale nonlinear programming," *Mathematical Programming*, vol. 106, no. 1, pp. 25–57, 2006.

Manuel Soler is an Assistant Professor in the area of Aerospace Engineering at the Universidad Carlos III de Madrid. He has been a visiting scholar in the Automatic Control Laboratory at the Swiss Federal Institute of Technology, ETH Zürich, Switzerland, and in the Institute of Transportation Studies at University of California Berkeley, USA. His research interests focus on optimal control, hybrid systems, and stochastic processes with application to aircraft trajectory planning in Air Traffic Management (ATM). He is member of the SESAR WP-E research network HALA! (Higher Levels of Automation in ATM). He has been awarded with the SESAR young scientist award 2013.

Maryam Kamgarpour is a postdoctoral fellow in the Automatic Control Laboratory at the Swiss Federal Institute of Technology, ETH Zürich. She completed her Ph.D. in Mechanical Engineering at the University of California, Berkeley (2011). Her research is on safety verification and optimal control of large scale uncertain dynamical systems with applications in air traffic and power grid systems. She is the recipient of NASA's High Potential Individual Award and NASA's Excellence in Publication Award and the European Union (ERC) Starting Grant 2015.

Javier Lloret is an Aeronautic Engineer (Masters Degree) at the Universidad Politecnica de Madrid (UPM). For one year was an Exchange Student at the Massachusetts Institute of Technology (MIT), focusing his studies in Aerodynamics and Structures. After finishing his Engineering studies, he enrolled in Aena (Spanish Air Navigation Service Provider) to become Air Traffic Controller. He currently holds all three possible endorsements (Tower, Approach and Enroute). He was assigned for more than two years in Valencia Tower and currently works in Madrid ACC. Since 2014, Javier Lloret is part-time faculty in the area of Aerospace Engineering at the Universidad Carlos III de Madrid, where he teaches graduate and undergraduate courses on air navigation and air transport.

John Lygeros is a Professor of Computation and Control at the Swiss Federal Institute of Technology (ETH) Zurich, Switzerland, since July 2006 and the Head of the Automatic Control Laboratory since January 2009. His research interests include modeling, analysis, and control of hierarchical, hybrid, and stochastic systems, with applications to biochemical networks, automated highway systems, air traffic management, power grids and camera networks. John Lygeros is a Fellow of the IEEE, and a member of the IET and of the Technical Chamber of Greece.